Colloids and Surfaces A: Physicochem. Eng. Aspects 368 (2010) 44–52

Contents lists available at ScienceDirect

Colloids and Surfaces A: Physicochemical and Engineering Aspects

journal homepage: www.elsevier.com/locate/colsurfa

Electroosmotic flow of power-law fluids at high zeta potentials

Nadapana Vasu, Sirshendu De*

Department of Chemical Engineering, Indian Institute of Technology, Kharagpur 721302, West Bengal, India

ARTICLE INFO

Article history:
Received 10 May 2010
Received in revised form 9 July 2010
Accepted 13 July 2010
Available online 21 July 2010

Keywords:
Electroosmotic flow
Zeta potential
Flow behavior index
Electric double layer
Power-law fluid

ABSTRACT

In this paper, a mathematical model for electroosmotic flow of power-law fluids in a rectangular microchannel at high zeta potential is analyzed. The electric double layer (EDL) potential distribution is considered without Debye Huckel linear approximation. Numerical solution is obtained to analyze the fluid flow behavior. Parametric studies are conducted to assess the variation of shear stress, viscosity and volumetric flow rates of various values of flow behavior index (n). Computed results are used to explicate the possibility of using a relatively pseudoplastic fluid inside microchannel to obtain higher volumetric flow rates.

1. Introduction

The advent of microfluidic devices in various areas of scientific research is due to their versatile features like, high surface-to-volume ratio, high rates of heat and mass transport leading to better separations, reactions, detections and high safety [1–6]. The various applications of microfluidic devices range from microreactors [7–10], heat transfer in electronic circuits [11,12], micro-total analysis systems (μTAS) involving DNA analysis and sequencing, bio-sensors, drug delivery [13–16], etc. In these applications, a wide variety of fluids ranging from simple electrolyte solutions to complex cell suspensions and polymer melts are dealt. Hence, in order to achieve better manipulation and control over fluid flow of such variety of fluids inside a microfluidic device, an in depth understanding of the transport process involved in microscales is essential. Electroosmotic flow (EOF) is the flow induced by the application of electric field across the channel and due to the presence of EDL at the channel wall [17]. The growing importance to the electroosmotic flow in the field of microfluidics is due to their operational advantages, like, plug flow type flow behavior, negligible axial dispersion, absence of mechanical pumping equipments and better flow control.

Several researchers have investigated various aspects of EOF in microchannels [18–33]. In most of the works, electrostatic potential distribution of EDL in microchannel is obtained by solving Poisson–Boltzmann equation with Debye Huckel linear approximation. Hence, above analyses are expected to be valid only in case of low zeta potentials (i.e., $\left|ze\zeta/k_BT\right| \leq 1$, for a symmetric electrolyte). However, in course of time, zeta potential in microchannel is being used as an important parameter to facilitate transport and separation of species [34]. It is possible to alter the zeta potential in a microchannel as desired by means of changing electrolyte concentrations, adding surfactants and by polymeric coatings on surface [35–37]. Hence it is extremely realistic to have zeta potentials ($\left|\zeta\right|$) as high as 100 mV inside a microchannel and in such cases Debye Huckel linear approximation fails to provide accurate electrostatic potential distribution. However, most of research works reported are limited by Debye Huckel linear approximation. Relatively few works are available on application of high zeta potentials in microchannels without Debye Huckel linear approximation [20–22,34,38–40]. Some of the most remarkable works related to high zeta potentials in microchannels are mentioned below. Levine et al. [20] was the first to study electrokinetic flow in cylindrical capillaries without Debye Huckel linear approximation. The analysis is performed satisfactorily using approximation given by Philip and Wooding (in obtaining EDL potential distribution around a charged cylindrical particle in an electrolyte) [41]. In 1975, Levine et al. [21] analyzed the electrokinetic flow in a narrow parallel plate channel. An analytical expression for electric potential in the form of a rapidly converging infinite series is obtained providing robust analysis without Debye Huckel linearization. Dutta and Beskok [22] studied the combined electroosmotic (EOF) and pressure driven flows (PDF) in microchannel beyond Debye Huckel approximation (DH approximation). Electrokinetic transport of solutes in nano-channels for high zeta potentials is analyzed by Pennathur and Santiago [38]. Effect of streaming potential on solute dispersion in nano-channels is studied by Xuan [39]. In that work, electric potential distribution is given as an elliptical function of

* Corresponding author. Tel.: +91 3222 283926; fax: +91 3222 255303.
E-mail address: sde@che.iitkgp.ernet.in (S. De).

0927-7757/$ – see front matter © 2010 Elsevier B.V. All rights reserved.
doi:10.1016/j.colsurfa.2010.07.014

Nomenclature

C	Concentration (kg/m^3)
E_x	Electric field strength (V/m)
F	Body force term
F_x	x-component of body force term
Q	Volumetric flow rate of power-law fluid (m^3/s)
Q_o	Volumetric flow rate of Newtonian fluid (m^3/s)
T	Absolute temperature (K)
e	Electron charge, 1.6×10^{-19} C
h	Half height of channel (m)
k_B	Boltzmann constant, 1.3805×10^{-23} J mol^{-1} K^{-1}
m	Flow consistency index, 0.9×10^{-3} Pa s
n	Flow behavior index
n_o	Number concentration of electrolyte
v_x	Velocity in axial direction (m/s)
v_{avg}	Average velocity (m/s)
v_s	Generalized Smoluchowski velocity of power-law fluid (m/s)
v_{so}	Smoluchowski velocity of Newtonian fluid (m/s)
w	Width of microchannel (m)
x	Axial co-ordinate
y	Transverse co-ordinate
z	Valency of the electrolyte

Greek Symbols

α	Parameter in Eq. (9)
ε	Dielectric constant of the medium, dimensionless
ε_o	Permitivity of vacuum, 8.854×10^{-12} C V^{-1} m^{-1}
ζ	Zeta potential (V)
κ^{-1}	EDL thickness (m)
μ	Viscosity of the power-law fluid (Pa s^{-n})
μ_o	Viscosity of the Newtonian fluid (Pa s)
μ_{ws}	Viscosity of the power-law fluid at channel wall (Pa s^{-n})
ρ	Charge density (C m^{-3})
ρ_f	Density of fluid (kg m^{-3})
τ	Shear stress (Pa)
τ_{ws}	Wall Shear stress (Pa)
Ψ	Electrostatic potential across the channel (V)

potential at centre and transverse axis co-ordinate. An iterative algorithm to find the potential at centre of microchannel based on zeta potential is presented [39]. Dutta [34] studied the transport of charged solutes in micro- and nano-fluidic channels at high zeta potentials. The effect of zeta potential on solute transport is described in detail. Recently, Elazhary and Soliman [40] theoretically studied the fluid flow and heat transfer during pressure driven flow at high zeta potentials.

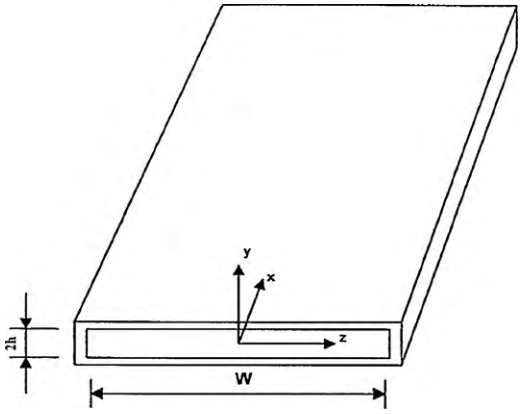

Fig. 1. Schematic diagram of a rectangular microchannel (height $2h$; width w).

All the above mentioned research works are confined to Newtonian fluid flow in microchannels. However, flows present in micro- and nano-channels are not always Newtonian in nature. There are comparatively few works reported in the literature characterizing the non-Newtonian fluid flow in microchannels [42–50]. The available works on this topic are summarized in Table 1. According to knowledge of authors, majority of works available in non-Newtonian rheology are confined to DH approximation and fails to explain flows in case of high zeta potentials. Thus, it is evident that there is necessity of research to be carried out in analysis of non-Newtonian flows in microchannels without DH approximation.

In this work, a detailed analysis of flow behavior of power-law fluids subjected to electroosmotic forces in a rectangular microchannel is undertaken. It is emphasized that the present work is not limited by Debye Huckel linear approximation and strongly applicable to characterize electroosmotic flow of power-law fluids in microchannels. Accurate prediction of non-Newtonian flow behavior at high zeta potentials is the novelty of this present work. Velocity profiles of various values of flow behavior index (n) are obtained. The obtained numerical solutions of velocity profiles are compared with analytical solutions presented by Zhao et al. [44] at low zeta potentials and are found to be in good agreement. Effects of electrokinetic radius (κh), flow behavior index (n), applied electric field, zeta potential on shear stress, viscosity and volumetric flow rate during electroosmotic flow of power-law fluids are analyzed.

2. Theory

2.1. Geometry description

Consider a microchannel between two parallel plates separated by a distance of '$2h$'. The system geometry is sketched in Fig. 1. The channel wall is considered to have uniform surface charge and hence a uniform zeta potential (ζ) exists at the stern layer

Table 1
Studies on non-Newtonian fluid flow in microchannels.

Reference	Theory	Experiments	Fluid flow	Electric potential
Das and Chakraborty [42]	Power-law, u, C, T		Pure EOF	With DH approximation
Chakraborty [43]	Power-law, u		Pure EOF	With DH approximation
Zhao et al. [44]	Power-law, u		Pure EOF	With DH approximation
Berli and Olivares [45]	Power-law, u		EOF + PDF	With DH approximation
Tang et al. [46]	Power-law, u		Pure EOF	Lattice Boltzmann method
Afonso et al. [47]	Viscoelastic, u		EOF + PDF	With DH approximation
Bharti et al. [48]	Power-law, u		PDF	Numerical solution
Berli [49]	Power-law, Q	Comparison	EOF + PDF	With DH approximation
Tang et al. [50]	Power-law, u		PDF	Lattice Boltzmann method
Present work	Power-law, u		EOF	High zeta potentials, without DH approximation

of the EDL. It is assumed that the fluid is continuous and isothermal (negligible Joule heating effects). The dielectric constant (ε) of the medium is constant and uniform everywhere inside the flow domain.

A steady, laminar, fully developed flow of an incompressible power-law fluid containing symmetric electrolyte, subjected to electroosmotic flow is considered for investigation. Under the above mentioned flow conditions, the elastic effects are negligible and the dominant factor is the viscosity which depends upon shear rate.

2.2. Power-law fluids

In non-Newtonian fluids, the viscous stress is a non-linear function of shear rate or velocity gradient (dv_x/dy). The rheology of fluid under investigation here is described by the power-law model (also known as the Ostwald-de Waele model). A power-law fluid is a generalized non-Newtonian fluid whose viscosity (μ) is given as:

$$\mu = m\left|\frac{dv_x}{dy}\right|^{n-1} = \mu = m\left(-\frac{dv_x}{dy}\right)^{n-1} \tag{1}$$

where, m is the flow consistency index, n is the flow behavior index. The negative sign is incorporated because the velocity decreases with increase in y.

The shear stress (τ) of a power-law fluid is given as:

$$\tau = m\left(-\frac{dv_x}{dy}\right)^{n-1}\frac{dv_x}{dy} \tag{2}$$

The indices m, n depends on ionic strength, pH and temperature of the fluid. The power-law fluids are classified based on the flow behavior index n.

2.3. Governing equations for fluid flow

A fully developed laminar flow of incompressible power-law fluid is induced in the microchannel by application of electric field across the channel causing electroosmotic flow (EOF). The flow is driven by the electric body force generated due to the presence of EDL at the channel wall. The body force is generated due to the interactions of net charge density (ρ) in EDL and the applied electric field strength, E_x (V/m). The electric field here is an operating condition.

The Navier–Stokes equation which is derived from equation of motion by assuming constant density is used to define the fluid flow and is given as:

$$\rho_f\frac{D}{Dt}v = -\nabla.\tau + F \tag{3}$$

where, ρ_f is the density of fluid and F is the body force term.

The electric body force on the EDL due to applied electric field in axial direction is given as:

$$F_x = \rho E_x \tag{4}$$

As the flow is electroosmotically driven, there is no applied pressure and gravitational body force. The electric potential distribution developed due to the presence of EDL in a rectangular microchannel, described by the Poisson equation is given as:

$$\frac{d^2\psi}{dy^2} = -\frac{\rho}{\varepsilon\varepsilon_o} \tag{5}$$

where, Ψ is the potential distribution of EDL, ε is the dielectric constant of medium and ε_o is the permittivity of vacuum $=8.854\times10^{-12}\,\mathrm{C\,V^{-1}\,m^{-1}}$. The charge density in EDL is given by the Boltzmann distribution with following assumptions: (i) ions are point charges and (ii) permittivity of fluid is constant and not affected by overall field strength:

$$\rho = \sum nze = -2n_o ze\,\sinh\left(\frac{ze\psi}{k_BT}\right) \tag{6}$$

$$\frac{d^2\psi}{dy^2} = -\frac{2n_o ze}{\varepsilon\varepsilon_o}\,\sinh\left(\frac{ze\psi}{k_BT}\right) \tag{7}$$

The above differential equation is subject to boundary conditions:

$$\text{At } y = 0\ \frac{d\psi}{dy} = 0 \tag{8a}$$

$$\text{At } y = h\ \psi = \zeta \tag{8b}$$

where, n_o is the bulk number concentration, z is the valency of ions, e is charge of an electron (1.6×10^{-19} C), k_B is the Boltzmann constant, T is the absolute temperature of the system.

The solution for electric potential distribution in a rectangular microchannel is given as [51]:

$$\psi = \frac{4\zeta}{\alpha}\,\tan h^{-1}\left[\tan h\left(\frac{\alpha}{4}\right)\exp(\kappa y - \kappa h)\right] \tag{9}$$

where, $\alpha = ze\zeta/k_BT$ and $\kappa^2 = 2n_oz^2e^2/€€_ok_BT$, κ^{-1} is the Debye length or thickness of EDL, respectively. The above expression for potential distribution is obtained by assuming that the EDL potential dies out at the center of microchannel i.e., the case of thin EDL ($\kappa h \geq 1$). Hence this entire analysis is valid for high zeta potentials but without EDL overlap.

The modified Navier–Stokes equation incorporating the electric body force term (simplified from Eq. (3)) is given as:

$$\frac{d}{dy}\left[m\left(-\frac{dv_x}{dy}\right)^{n-1}\frac{dv_x}{dy}\right] - \varepsilon\varepsilon_oE_x\frac{d^2\psi}{dy^2} = 0 \tag{10}$$

The above equation is subjected to the following boundary conditions:

$$\text{At } y = 0\ \frac{dv_x}{dy} = 0 \tag{11a}$$

$$\text{At } y = h\ v_x = 0 \tag{11b}$$

Integrating Eq. (10) and subject to boundary condition Eqs. (8a) and (11a) gives:

$$\left(-\frac{dv_x}{dy}\right) = \left[-\frac{\varepsilon\varepsilon_oE_x}{m}\frac{d\psi}{dy}\right]^{1/n} \tag{12}$$

Integrating Eq. (7) subject to boundary conditions in Eqs. (8a) and (8b), the following expression is resulted:

$$\frac{d\psi}{dy} = \kappa\left(\frac{2\zeta}{\alpha}\right)\,\sinh\left(\frac{\alpha\psi}{2\zeta}\right) \tag{13}$$

From Eq. (12), the velocity gradient of the power-law fluid is given as:

$$\frac{dv_x}{d} = -\left[-\frac{\kappa\varepsilon\varepsilon_oE_x\zeta}{m}\right]^{1/n}\left[\frac{2}{\alpha}\,\sinh\left(\frac{\alpha\psi}{2\zeta}\right)\right]^{1/n} \tag{14}$$

The expression for viscosity of power-law fluids is given as:

$$\mu = m\left(-\frac{dv_x}{dy}\right)^{n-1}$$

$$= m^{1/n}(-\kappa\varepsilon\varepsilon_oE_x\zeta)^{(n-1)/n}\left[\frac{2}{\alpha}\,\sinh\left(\frac{\alpha\psi}{2\zeta}\right)\right]^{(n-1)/n} \tag{15}$$

The shear stress distribution can be given as:

$$\tau_{yx} = -m\left(-\frac{dv_x}{dy}\right)^n \tag{16}$$

By putting $\psi = \zeta$ and $y = h$ in Eqs. (15) and (16), the wall shear stress (τ_{ws}) and dynamic viscosity of power-law fluid at channel wall (μ_{ws}) are given as:

$$\tau_{ws} = \frac{2\kappa\varepsilon\varepsilon_o E_x\zeta}{\alpha}\ \sinh\left(\frac{\alpha}{2}\right) \tag{17}$$

$$\mu_{ws} = m^{1/n}(-\kappa\varepsilon\varepsilon_o E_x\zeta)^{(n-1)/n}\left[\frac{2}{\alpha}\ \sinh\left(\frac{\alpha}{2}\right)\right]^{(n-1)/n} \tag{18}$$

The velocity distribution of electroosmotic flow of power-law fluids is obtained by integrating Eq. (14) subject to boundary condition Eq. (11b) and is given as:

$$v_x(y) = \kappa^{(1-n)/n}\left[-\frac{\varepsilon\varepsilon_o E_x\zeta}{m}\right]^{1/n}\int_{\kappa y}^{\kappa h}\left[\frac{2}{\alpha}\ \sinh\left\{2\ \tan\ h^{-1}\left(\tan\ h\left(\frac{\alpha}{4}\right)\ \exp\left(\kappa y - \kappa h\right)\right)\right\}\right]^{1/n} d(\kappa y) \tag{19}$$

The expression for average velocity (v_{avg}) is given as:

$$v_{avg} = \frac{\kappa^{(1-n)/n}}{h}\left[-\frac{\varepsilon\varepsilon_o E_x\zeta}{m}\right]^{1/n}\int_0^h\left(\int_{\kappa y}^{\kappa h}\left[\frac{2}{\alpha}\ \sinh\left\{2\ \tan\ h^{-1}\left(\tan\ h\left(\frac{\alpha}{4}\right)\ \exp\left(\kappa y - \kappa h\right)\right)\right\}\right]^{1/n} d(\kappa y)\right) dy \tag{20}$$

The volumetric flow rate (Q) is given as:

$$Q = 2\,v_{avg}hw \tag{21}$$

where, w is the width of the microchannel. The expressions for velocity distribution, viscosity, average velocity (Eqs. (15)–(21)) boils down to the expressions given by Zhao et al. [44], under Debye Huckel linear approximation i.e., the case with low surface potentials ($|\zeta| < 25.4$ mV). Hence, the present analysis is strongly applicable to characterize electroosmotic fluid flow behavior in high zeta potential microfluidic systems.

3. Results and discussion

In the previous section, general expressions concerning the EDL electric potential, velocity fields, viscosity, etc., are presented. Here in this section, a detailed discussion of the numerical solutions obtained is attempted providing new and interesting physical insight into non-Newtonian fluid flow in microdevices. A parallel plate microchannel made of silicon (having negative zeta potential) is considered for analysis. The dimensions of microchannel are length 5×10^{-2} m, width 300 μm and height 100 μm. The working fluids are a range of power-law fluids containing monovalent symmetric electrolyte such as KCl or NaCl. The other parameters employed are: dielectric constant of medium, $\epsilon = 80$, permittivity of vacuum, $\epsilon_o = 8.85 \times 10^{-12}$ C V^{-1} m^{-1}, absolute temperature of system, $T = 300$ K, valency of ions, $z = 1$, wall zeta potential, $\zeta = -100$ mV, flow consistency index, $m = 0.9 \times 10^{-3}$ Pa s^n.

3.1. Verification of numerical solution:

To ensure accuracy of the computed numerical solution, the numerical solution computed in this present work is compared with analytical results presented by Zhao et al. [44] under Debye Huckel limit. It is already emphasized that, for low zeta potential systems, the Eqs. (15)–(21) of present work reduces to standard analytical expressions obtained by Zhao et al. [44]. Analytical solutions of velocity distribution using Debye Huckel linear approximation for $n = 1, 1/2, 1/3$ are obtained by Zhao et al. [44] and are as follows:

For $n = 1$

$$v_x(y) = -\frac{\varepsilon\varepsilon_o E_x\zeta}{m}\left[1 - \frac{\cosh(\kappa y)}{\cosh(\kappa h)}\right] \tag{22a}$$

For $n = \frac{1}{2}$

$$v_x(y) = \frac{1}{2}\kappa\left(-\frac{\varepsilon\varepsilon_o E_x\zeta}{m}\right)^2\frac{[\sinh(2\kappa h) - \sinh(2\kappa y) - 2(\kappa h - \kappa y)]}{2\ \cosh^2(\kappa h)} \tag{22b}$$

For $n = \frac{1}{3}$

$$v_x(y) = \frac{1}{3}\kappa^2\left(-\frac{\varepsilon\varepsilon_o E_x\zeta}{m}\right)^3 \times \frac{[\sinh(3\kappa h) - \sinh(3\kappa y) + 9\ \sinh(\kappa h) - 9\ \sinh(\kappa y)]}{4\ \cosh^3(\kappa h)} \tag{22c}$$

$$v_{avg} = n\kappa^{(1-n)/n}\left(-\frac{\varepsilon\varepsilon_o E_x\zeta}{m}\right)^{1/n} \times \frac{\frac{1}{2^{1/n}}\left[\left(1 - \frac{n}{\kappa h}\right)e^{(\kappa h)/n} + \frac{n-1}{\kappa h}e^{1/n}\right] + \frac{1}{\kappa h(1+2n)}}{\cosh^{1/n}(\kappa h)} \tag{22d}$$

The generalized Smoluchowski velocity for power-law fluids is given as:

$$v_s = n\kappa^{(1-n)/n}\left(-\frac{\varepsilon\varepsilon_o E_x\zeta}{m}\right)^{1/n} \tag{22e}$$

From Fig. 2, it can be inferred that the analytical solutions of Zhao et al. [44] are in good agreement with the numerical solution of the present work at lower zeta potential and hence the present work can accurately predict the behavior of high zeta potential systems. The numerical integration is carried out using Simpson's rule which has accuracy of order 10^{-6}.

3.2. Characteristics of electroosmotic flow of power-law fluids

The velocity distribution of electroosmotic flow of power-law fluids is obtained by numerical integration of Eq. (19). Fig. 3 shows the velocity distribution of various power-law fluids normalized with their respective average velocities (obtained from Eq. (20)) across the channel half height. For pseudo plastics ($n < 1$), the shear thinning nature reduces the maximum velocity and increases the velocity in a region very near to the channel wall leading to plug like behavior. Conversely for $n > 1$, the liquid is shear thickening

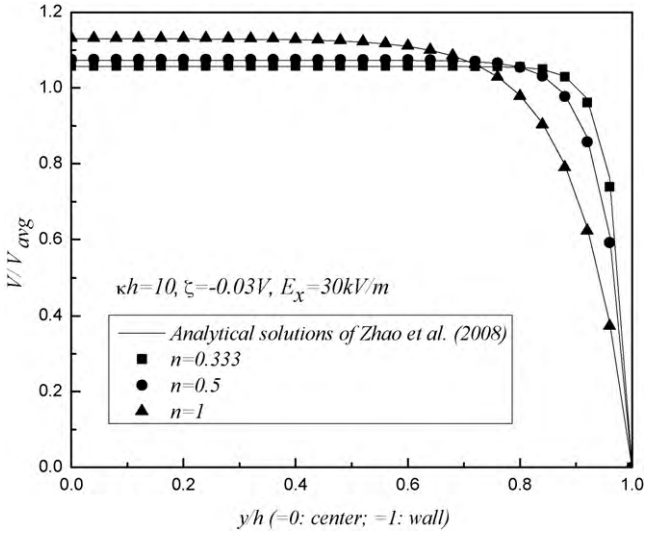

Fig. 2. Comparison of velocity profiles of present work with analytical expressions of Zhao et al. [44].

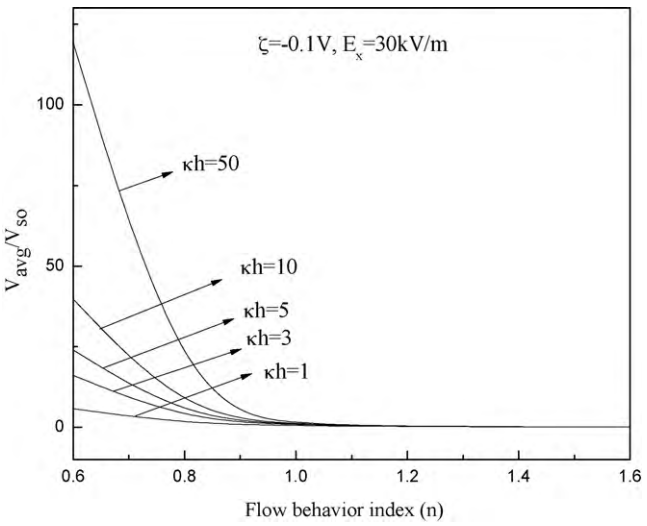

Fig. 4. Variation of average velocity of power-law fluids normalized with Smoluchowski velocity of Newtonian fluid with flow behavior index (n).

in nature and posses a maximum velocity at center leading to parabolic velocity profile. The maximum velocity increases with the flow behavior index (n).

The average velocity of power-law fluids is given by Eq. (20). Fig. 4 shows the average velocity of power-law fluids (v_{avg}) normalized with Smoluchowski velocity of Newtonian fluid ($v_{so} = -\varepsilon\varepsilon_o E_x\zeta/m$) and its variation with flow behavior index (n) at various EDL thicknesses. Here, The Smoluchowski velocity (v_{so}) is used as a reference velocity to compare the increase in magnitude of velocity of power-law fluids compared to Newtonian one. The average velocity of pseudo plastics ($n < 1$) is many times higher than that of conventional Smoluchowski velocity. This behavior is more predominant in thin EDL. Thus an increase in fluid velocity inside the microfluidic device is possible by altering the flow behavior index (n) of the working fluid (precisely making it slightly pseudo plastic). Flow behavior index (n) having dependence on temperature, pH and ionic strength is easy to manipulate. Also, average velocity is high at thin EDL. This can be obtained by using a relatively larger sized channel for same electrolyte concentration or using more electrolyte concentration for same channel size.

Fig. 5 shows the average velocity (using Eq. (20)) normalized by the generalized Smoluchowski velocity of various power-law fluids (using Eq. (22e)) at various EDL thicknesses. It is observed that the pseudoplastics ($n < 1$) posses higher average velocity. Hence, fraction of average velocity to Smoluchowski velocity is greater than 1 for pseudoplastics and reaches close to 1 with increase in the flow behavior index (n). The difference between average velocity and Smoluchowski velocity vanishes at thin EDL and is predominant in case of thicker EDL.

Fig. 6 shows the shear stress, τ (using Eq. (16)) distribution normalized with wall shear stress, τ_{ws} (using Eq. (17)) across the channel half height at various EDL thicknesses. The shear stress distribution is independent of the flow behavior index n. For $\kappa h > 1$, the shear stress at the center of channel is zero and increases to wall shear stress (τ_{ws}) at the channel wall. For thicker EDL, the driving force is confined to entire channel half height and hence there is gradual variation of shear stress across the channel half height. For thin EDL ($\kappa h = 50$), the driving force rests very close to the walls and hence the shear stress is zero over most of half height and exponentially increases to wall shear stress at channel wall.

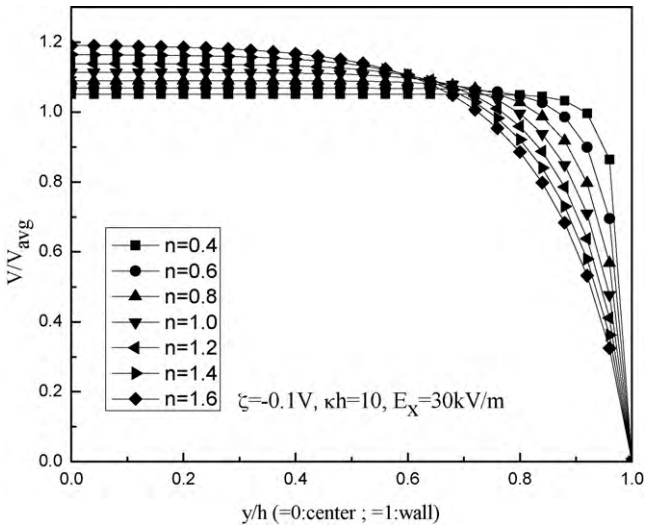

Fig. 3. Velocity profiles of power-law fluids normalized with average velocity across the microchannel.

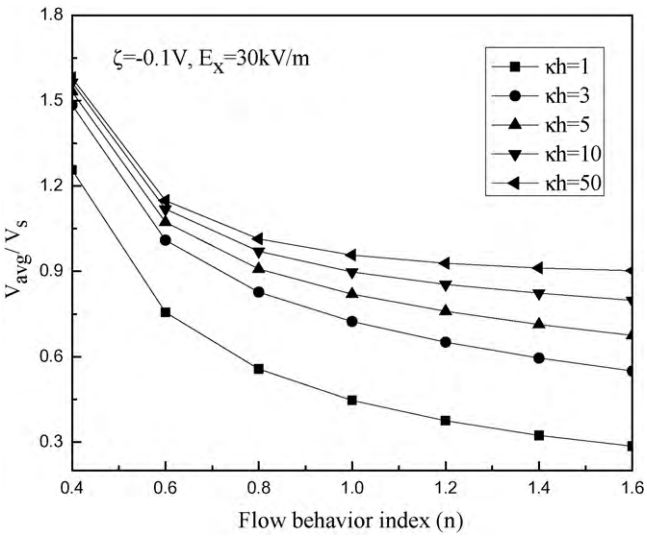

Fig. 5. Variation of average velocity normalized with generalized Smoluchowski velocity with flow behavior index (n).

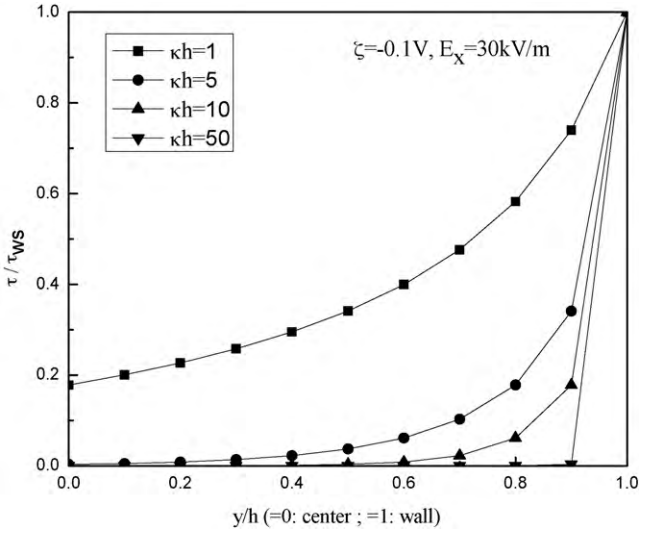

Fig. 6. Normalized shear stress profiles across the channel for various κh.

The dynamic viscosity μ and dynamic viscosity at channel wall μ_{ws} are calculated from Eqs. (15) and (18) respectively. Fig. 7 shows the profiles of fluid viscosity (μ) normalized with viscosity at wall (μ_{ws}) across the channel half height for various values of flow behavior index n. Unlike Newtonian fluids, the viscosity of power-law fluids is dependent on position across the channel. Also, irrespective of flow behavior index, dimensionless viscosity reaches 1 near channel wall. For shear thinning fluid or pseudoplastics ($n < 1$), viscosity is infinite at channel center due to absence of velocity gradient and decreases to dynamic viscosity at channel wall. For $n = 1$, the viscosity is constant at entire cross-section and is equal to dynamic viscosity at wall. For shear thickening or dilatant fluids ($n > 1$), viscosity is zero at center of channel (inviscid) due to absence of velocity gradient and increases to dynamic viscosity at wall.

The variation of dynamic viscosity at channel wall (μ_{ws}) for various values of flow behavior index, n is presented in Fig. 8a and b with reference to Newtonian fluid viscosity (μ_o). The dynamic viscosity evaluated using Eq. (18) is dependent on flow behavior index n, electrokinetic radius κh and applied electric field strength E_x.

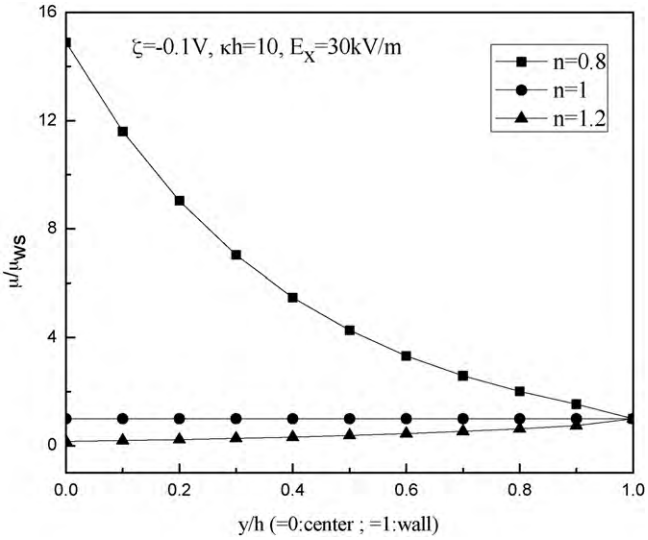

Fig. 7. Dimensionless dynamic viscosity profile across the channel for various values of flow behavior index (n).

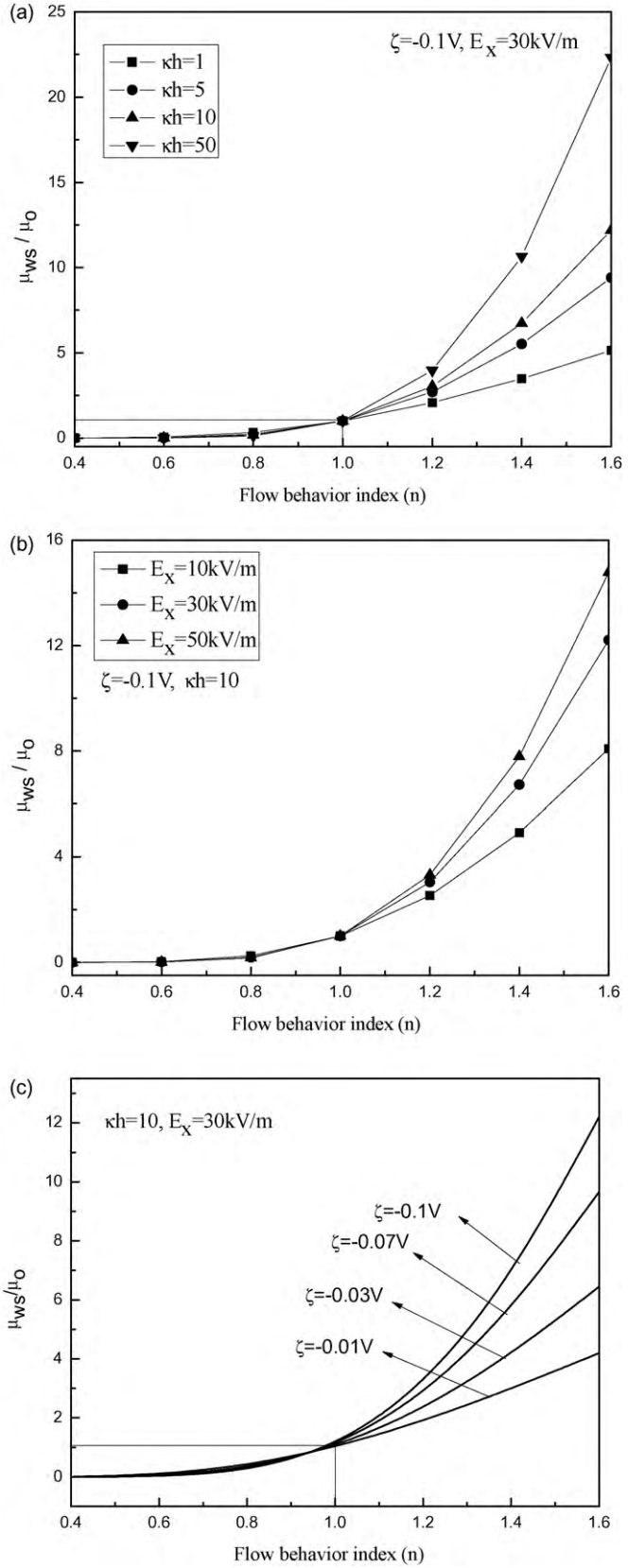

Fig. 8. (a) Variation of dynamic viscosity at channel wall (μ_{ws}) normalized with Newtonian fluid viscosity (μ_o) with EDL thickness for various values of flow behavior index (n). (b) Variation of dynamic viscosity at channel wall (μ_{ws}) normalized with Newtonian fluid viscosity (μ_o) with applied electric field for various values of flow behavior index (n). (c) Variation of dynamic viscosity at channel wall (μ_{ws}) normalized with Newtonian fluid viscosity (μ_o) with zeta potential for various values of flow behavior index (n).

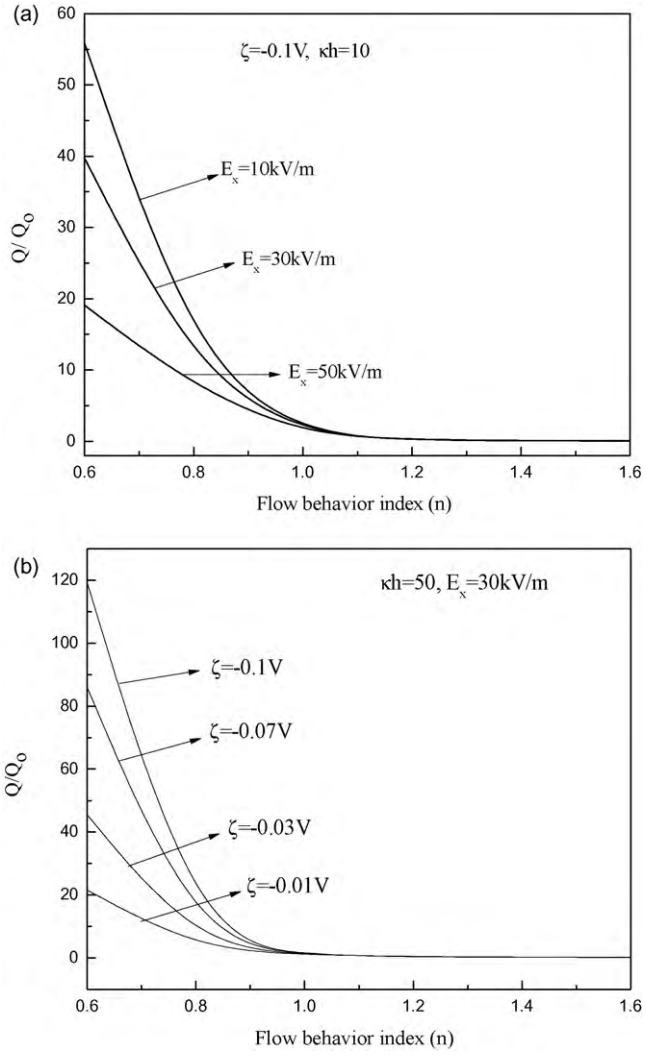

Fig. 9. (a) Effect of applied electric field on dimensionless volumetric flow rate for various values of flow behavior index (n). (b) Effect of zeta potential on dimensionless volumetric flow rate for various values of flow behavior index (n).

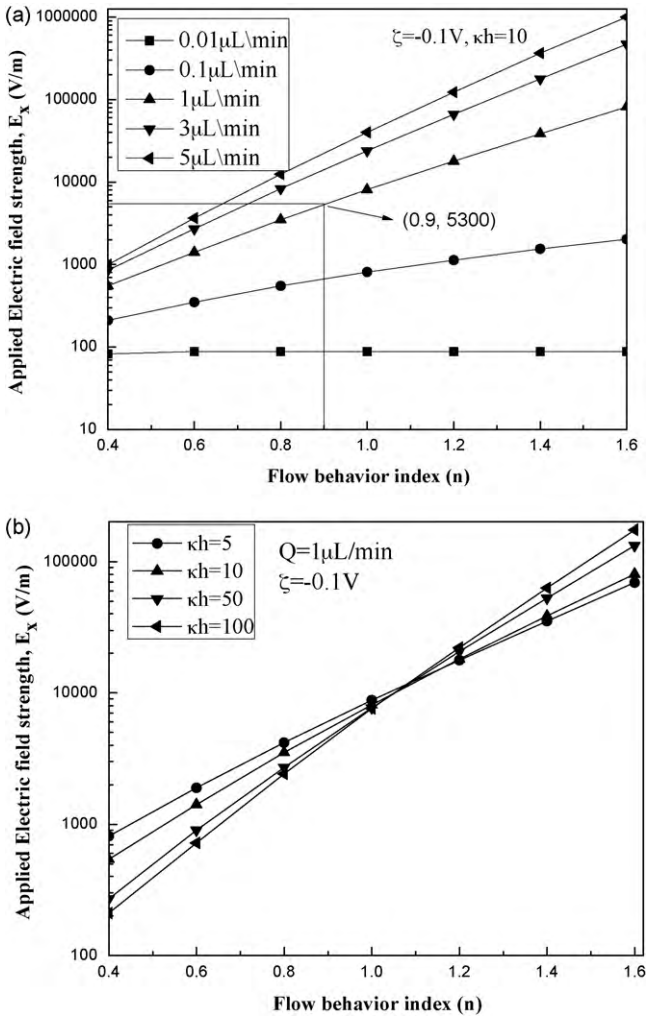

Fig. 10. (a) Variation of electric field to be applied (E_x) for various values of flow behavior index (n) in order to achieve constant volumetric flow rate inside a microchannel. (b) Variation of amount of applied electric field (E_x) for various values of flow behavior index (n) in order to achieve 1 μL\min volumetric flow rate with different electrolyte concentrations.

The dynamic viscosity at channel wall increases with flow behavior index. The variation with electrokinetic radius κh is presented in Fig. 8a. For pseudo plastics ($n < 1$), the variation is negligible. For Newtonian fluids, the ratio μ_{ws}/μ_o becomes 1 and for dilatant fluids, the dynamic viscosity at channel wall increases with κh (i.e., more for thin EDL).

Fig. 8b shows the dependence of dynamic viscosity at channel wall of various power-law fluids on applied electric field strength E_x. The dependence is negligible for pseudoplastics ($n < 1$) and for dilatants, increase in electric field strength increases the viscosity at channel wall. Fig. 8c shows the dependence of dynamic viscosity at channel wall of various power-law fluids on zeta potential. The dynamic viscosity of channel wall increases with zeta potential. The dependence is negligible for pseudoplastics ($n < 1$) and predominant in dilatants ($n > 1$).

Fig. 9a shows the affect of applied electric field on dimensionless volumetric flow rate for various values of flow behavior index n. The volumetric flow rate (Q) is obtained from Eq. (20) and the reference flow rate (Q_o) is that of a Newtonian fluid. It is inferred that the volumetric flow rate of pseudoplastics ($n < 1$) are many times that of Newtonian fluid. Also, increase in applied electric field strength increases the volumetric flow rate. For dilatant fluids, the volumetric flow rates decrease with flow behavior index as low to 10% of Newtonian fluid volumetric flow rate (Q_o). This is because of high viscosity of the shear thickening fluids. Also, application of high external electric field does not ensure increase in volumetric flow rates of dilatant fluids.

In Fig. 9b, the affect of zeta potential on dimensionless volumetric flow rate for various values of flow behavior index n is studied. It is observed that the volumetric flow rate of pseudoplastics ($n < 1$) is many times that of a Newtonian fluid. Also, the volumetric flow rate of pseudoplastics increases with increase in magnitude of zeta potentials. However, the effect of zeta potential on flow rates of dilatants fluids (shear thickening fluids) inside a microfluidic device is negligible. Hence, it is practically difficult to ensure and control flow of shear thickening fluids inside a microfluidic device. It is desirable to slightly alter the flow behavior index of the working fluid inside microfluidic device so as to ensure high volumetric flow rates. Microfluidic devices which facilitate high heat and mass transport rates become more advantageous with high throughput (volumetric flow rates) for same amount of driving force (either pressure driven or electric driven). In other words, it can be said that lesser driving force is required to attain same amount of volumetric flow rates.

Fig. 10a shows the amount of electric field E_x to be applied for various power-law fluids to attain a constant volumetric flow rate

inside a microfluidic device. The amount of electrolyte concentration, C is maintained constant at 3.5×10^{-9} M ($\kappa h = 10$). In order to obtain a fixed volumetric flow rate, amount of electric field to be applied, E_x increases with increase in flow behavior index value. This is because of increase in fluid viscosity. Also in order to achieve a volumetric flow rate of 1 μL/min inside a microfluidic device, by slightly modifying the flow behavior index of working fluid to say $n = 1$ to $n = 0.9$, the amount of electric field to be applied decreases from 8100 to 5300 V/m, a reduction in 33% of necessary field strength which is highly desirable.

Fig. 10b shows the amount of electric field to be applied for various power-law fluids to attain a constant volumetric flow rate of 1 μL/min at various electrolytic concentrations. It is observed that for pseudoplastics, the electric field required decreases with increase in EDL thickness (κh). This is because for pseudoplastics, the average velocity increases with EDL thickness (κh). Thus, in order to have 1 μL/min in case of a pseudoplastic, for low κh more electric field strength has to be applied compared with large κh. For dilatant fluids, the amount of electric field to be applied increases with increase in EDL thickness (κh). This is because, the average velocity decreases with EDL thickness in such fluids.

4. Conclusion

Electroosmotic flow of power-law fluids in a rectangular microchannel is studied theoretically at high zeta potentials. It is observed that the pseudoplastics have higher average velocity in microchannel than that of dilatants, for same operating conditions. Hence, in order to obtain more volumetric flow rate in a microfluidic device, one can opt for a suitable working fluid which is pseudoplastic in nature rather than increasing the magnitude of electric field to be applied. By changing the flow behavior index from $n = 1$ to $n = 0.9$, a reduction in 33% of field strength to be applied is successfully demonstrated. Apart from this, parametric studies are carried out to assess the effects of electrokinetic radius (κh), zeta potential (ζ) and applied field strength (E_x) as shear stress distribution, viscosity and volumetric flow rate during EOF of power-law fluids at high zeta potentials. This understanding helps in efficient design of fluid flow in a microfluidic device which has applications in site specific species transport such as drug delivery and species separation.

References

[1] G.E. Karniadakis, A. Beskok, N. Aluru, Microflows and Nanoflows: Fundamentals and Simulation, Springer, New York, 2005.
[2] W. Ehrfeld, V. Hessel, H. Lowe, Microreactors: New Technology for Modern Chemistry, Wiley-VCH, Weinheim, 2000.
[3] D. Erickson, D. Li, Integrated microfluidic devices, Anal. Chim. Acta 507 (2004) 11–26.
[4] H.A. Stone, A.D. Strook, A. Ajdari, Engineering flows in small devices: microfluidics toward a lab-on-a-chip, Annu. Rev. Fluid Mech. 36 (2004) 381.
[5] W. Ehrfeld, Electrochemistry and microsystems, Electrochim. Acta 48 (2003) 2857–2868.
[6] A.G. Hadd, D.E. Raymond, J.W. Halliwell, S.C. Jacobson, J.M. Ramsey, Microchip device for performing enzyme assays, Anal. Chem. 69 (1997) 3407–3412.
[7] H. Lowe, W. Ehrfeld, State of the art in microreaction technology: concepts, manufacturing and application, Electrochem. Acta 44 (1997) 3679–3689.
[8] O. Worz, K.P. Jackel, T. Richter, A. Wold, Microreactors, a new efficient tool for optimum reactor design, Chem. Eng. Sci. 56 (2001) 1029–1033.
[9] S.V. Gokhale, R.K. Tayal, V.K. Jayaraman, B.D. Kulkarni, Microchannel reactors: application and use in process development, Int. J. Chem. Reactor Eng. 3 (R2) (2005) 1–51.
[10] K.F. Jensen, Microreaction engineering-is small better? Chem. Eng. Sci. 56 (2001) 293–303.
[11] J. Koo, C. Kleinstreuer, Viscous dissipation effects in microtubes and microchannels, Int. J. Heat Mass Transf. 47 (2004) 3159–3169.
[12] V. Hessel, S. Hardt, H. Lowe, Chemical Micro Process Engineering: Fundamentals, Modeling and Reactions, Wiley-VCH, Weinheim, 2004.
[13] D.R. Reyes, D. Lossifidis, P. Auroux, A. Manz, Micro total analysis systems. 1. Introduction, theory and technology, Anal. Chem. 74 (2002) 2623–2636.
[14] J. Chen, M. Chu, K. Koulajian, X.Y. Wu, A. Giacca, Y. Sun, A monolithic polymeric microdevice for pH-responsive drug delivery, Biomed. Microdevices 11 (2009) 1251–1257.
[15] S.J. Lee, S.Y. Lee, Micro total analysis system (μ-TAS) in biotechnology, Appl. Microbiol. Biotechnol. 64 (2004) 289–299.
[16] A. Berg, T.S.J. Lammerink, Micro total analysis systems: microfluidic aspects, integration concept and applications, Top. Curr. Chem. 194 (1998) 22–49.
[17] R.J. Hunter, Foundations of Colloid Science, Vol. 2, Clarendon press, Oxford, 1989.
[18] D. Burgreen, F.R. Nakache, Electrokinetic flow in ultrafine capillary slits, J. Phys. Chem. 68 (1964) 1084–1091.
[19] C.L. Rice, R. Whitehead, Electrokinetic flow in a narrow cylindrical capillary, J. Phys. Chem. 69 (1965) 417–424.
[20] S. Levine, J.R. Marriott, G. Neale, N. Epstein, Theory of electrokinetic flow in fine cylindrical capillaries at high zeta-potentials, J. Colloid Interface Sci. 52 (1975) 136–149.
[21] S. Levine, J.R. Marriott, K. Robinson, Theory of electrokinetic flow in a narrow parallel-plate channel, J. Chem. Soc. Faraday Trans. 2 71 (1975) 1–11.
[22] P. Dutta, A. Beskok, Analytical solution of combined electroosmotic/pressure driven flows in two-dimensional straight channels: finite Debye layer effects, Anal. Chem. 73 (2001) 1979–1986.
[23] L. Ren, D. Li, Electoosmotic flow in heterogeneous microchannels, J. Colloid Interface Sci. 243 (2001) 255–261.
[24] D.G. Yan, C. Yang, X.Y. Huang, Effect of finite reservoir size on electroosmotic flow in microchannels, Microfluid Nanofluid 3 (2007) 333–340.
[25] R.J. Yang, L.M. Fu, Y.C. Lin, Electroosmotic flow in microchannels, J. Colloid Interface Sci. 239 (2001) 98–105.
[26] J. Wang, M. Wang, Z. Li, Lattice Poisson–Boltzmann simulations of electroosmotic flows in microchannels, J. Colloid Interface Sci. 296 (2006) 729–736.
[27] X. Xuan, D. Li, Electroosmotic flow in microchannels with arbitrary geometry and arbitrary distribution of wall charge, J. Colloid Interface Sci. 289 (2005) 291–303.
[28] Y. Gao, T.N. Wong, C. Yang, K.T. Ooi, Two-fluid electroosmotic flow in microchannels, J. Colloid Interface Sci. 284 (2005) 306–314.
[29] Y. Zhang, X.J. Gu, R.W. Barber, D.R. Emerson, An analysis of induced pressure fields in electroosmotic flows through microchannels, J. Colloid Interface Sci. 275 (2004) 670–678.
[30] C.M. Brotherton, R.H. Davis, Electroosmotic flow in channels with step changes in zeta potential and cross section, J. Colloid Interface Sci. 270 (2004) 242–246.
[31] L.M. Fu, J.Y. Lin, R.J. Yang, Analysis of electroosmotic flow with step change in zeta potential, J. Colloid Interface Sci. 258 (2003) 266–275.
[32] K. Horiuchi, P. Dutta, Joule heating effects in electroosmotically driven microchannel flows, Int. J. Heat Mass Transfer 47 (2004) 3085–3095.
[33] S. Chakraborty, Analytical solutions of Nusselt number for thermally fully developed flow in microtubes under a combined action of electroosmotic forces and imposed pressure gradients, Int. J. Heat Mass Transfer 49 (2006) 810–813.
[34] D. Dutta, Transport of charged samples in fluidic channels with large zeta potentials, Electrophoresis 28 (2007) 4552–4560.
[35] B.J. Kirby, E.F. Hasselbrink Jr., Zeta potential of microfluidic substrates: 1. Theory, experimental techniques, and effects on separations, Electrophoresis 25 (2004) 187–202.
[36] B.J Kirby, E.F. Hasselbrink Jr., Zeta potential of microfluidic substrates: 2. Data for polymers, Electrophoresis 25 (2004) 203–213.
[37] J. Hahm, A. Balasubramanian, A. Beskok, Flow and species transport control in grooved microchannels using local electrokinetic forces, Phys. Fluids 19 (2007) 013601.
[38] S. Pennathur, J.G. Santiago, Electrokinetic transport in nanochannels. 1. Theory, Anal. Chem. 77 (2005) 6772–6781.
[39] X. Xuan, Streaming potential effects on solute dispersion in nanochannels, Anal. Chem. 79 (2007) 7928–7932.
[40] A. Elazhary, H.M. Soliman, Analytical solutions of fluid flow and heat transfer in parallel-plate micro-channels at high zeta-potentials, Int. J. Heat Mass Transfer 52 (19–20) (2009) 4449–4458.
[41] J.R. Philip, R.A. Wooding, Solution of the Poisson–Boltzmann equation about a cylindrical particle, J. Chem. Phys. 52 (2) (1970) 953–959.
[42] S. Das, S. Chakraborty, Analytical solutions for velocity, temperature and concentration distribution in electroosmotic microchannel flows of a non-Newtonian bio-fluid, Anal. Chim. Acta 559 (1) (2006) 15–24.
[43] S. Chakraborty, Electroosmotically driven capillary transport of typical non-Newtonian biofluids in rectangular microchannels, Anal. Chim. Acta 605 (2007) 175–184.
[44] C. Zhao, E. Zholkovskij, J.H. Masliyah, C. Yang, Analysis of electroosmotic flow of power-law fluids in a slit microchannel, J. Colloid Interface Sci. 326 (2008) 503–510.
[45] C.L.A. Berli, M.L. Olivares, Electrokinetic flow of non-newtonian fluids in microchannels, J. Colloid Interface Sci. 320 (2008) 582–589.
[46] G.H. Tang, X.F. Li, Y.L. He, W.Q. Tao, Electroosmotic flow of non-Newtonian fluid in microchannels, J. Non-Newton. Fluid Mech. 157 (2009) 133–137.
[47] A.M. Afonso, M.A. Alves, F.T. Pinho, Analytical solution of mixed electroosmotic/pressure driven flows of viscoelastic fluids in microchannels, J. Non-Newton. Fluid Mech. 159 (2009) 50–63.

[48] R.P. Bharti, D.J.E. Harvie, M.R. Davidson, Electroviscous effects in steady fully developed flow of a power-law liquid through a cylindrical microchannel, Int. J. Heat Fluid Flow 30 (2009) 804–811.
[49] C.L.A. Berli, Output pressure and efficiency of electrokinetic pumping of non-Newtonian fluids, Microfluid Nanofluid 8 (2009) 197–207.
[50] G.H. Tang, P.X. Ye, W.Q. Tao, Electroviscous effect on non-Newtonian fluid flow in microchannels, J. Non-Newton. Fluid Mech. 165 (2010) 435–440.
[51] W.B. Russel, D.A. Saville, W.R. Schowalter, Colloidal Dispersions, Cambridge University Press, Cambridge, 1992.